ETH zürich

ETH Library

Flow around a square cylinder controlled by synthetic jet positioned at upstream surface

Conference Paper

Author(s):
Qu, Y.; Wang, J.J.

Publication date:
2018-10-05

Permanent link:
https://doi.org/10.3929/ethz-b-000279175

Rights / license:
In Copyright - Non-Commercial Use Permitted

This page was generated automatically upon download from the ETH Zurich Research Collection.
For more information, please consult the Terms of use.

FLOW AROUND A SQUARE CYLINDER CONTROLLED BY SYNTHETIC JET POSITIONED AT UPSTREAM SURFACE

Y. Qu, J. J. Wang[c]

Key Laboratory of Fluid Mechanics (Beihang University), Ministry of Education, Beijing 100191, China
[c]Corresponding author: Email: jjwang@buaa.edu.cn

KEYWORDS:
Main subjects: flow control
Fluid: separated flows
Visualization method(s): Particle Image Velocimetry
Other keywords: synthetic jet, square cylinder, vortex dynamics

ABSTRACT: *The flow characteristics around a square cylinder with a slot synthetic jet injected from its upstream surface is studied experimentally in a water channel using planar Particle Image Velocimetry (PIV) technique. The dimensionless excitation frequency is at a certain value of f_e/f_0=3.4, and the dimensionless stroke length is L_0/w=43.6. The differences of the flow dynamics upstream and downstream of the square cylinder are compared between the natural case and the controlled case. The phase-averaged and time-averaged methods are used to present the variation of flow structures. The Fourier mode decomposition (FMD) method is applied to obtain the frequency information of the flow field. For the controlled case, the synthetic jet always deflects to one side (either +y or -y direction) and does not change this deflecting direction. The synthetic jet vortices keep growing after generating at the slot exit and then lose their stability. The flow field at the upstream of the cylinder's rear surface is dominated by the excitation frequency due to the periodic disturbance of synthetic jet. With control, the separation of square cylinder is suppressed effectively for the side where the synthetic jet deflects. The wake becomes turbulent and no periodic wake vortex shedding is detected for the controlled case.*

1 Introduction

Flow over a square cylinder has attracted considerable attention of researchers due to its extensive engineering applications. Many architectures in daily life, such as tall buildings and bridge piers, can be simplified as square cylinders. As is known, when flow passes across a square cylinder, flow separates at the front corners and vortex shedding occurs in the wake, causing a series of problems such as flow induced vibrations, acoustic noise and drag and lift fluctuations [3], which can sometimes destroy the structures.

Various kinds of passive or active control methods have been reported by researchers to improve the aerodynamic characteristics of the square cylinder, including control rod, splitter plate, corner modification, plasma, oscillation, acoustic excitation, suction/blowing, jet, and so forth. Particularly, both the continuous jet and the synthetic jet issued from the downstream surface of the square cylinder have been proved to have good control effects on changing the vortex shedding modes, suppressing the periodic wake instabilities and reducing the drag force [1][4][8][9]. In addition, Huang, Hsu & Chiu [5] placed the planar jet at the upstream surface of a square cylinder. As the injection ratio increased, four characteristic flow modes were observed, and the drag coefficient decreased quickly. However, as a recently developed control method, the synthetic jet has been rarely considered to be placed at the upstream surface of a square cylinder to control the flow, the associated experiment is thus conducted in our present work to compare the flow behaviors for the natural case and a certain controlled case.

2 Experimental Set-up

The experiment was performed in a low-speed water channel with a working section of 600 mm × 600 mm × 3000 mm (height × width × length). The free-stream turbulence intensity Tu was less than 0.8%. A hollow square cylinder made of stainless steel was used as the experimental model, its side width D was 20 mm and its span length L was 430 mm. The cross-section of the square cylinder at its mid-span and the schematic of the experimental arrangement are shown in Fig. 1(a) and Fig. 1(b), respectively. Two end plates were used to reduce the three-dimensional end effects, which were caused by the boundary layer developing along the side walls of the water channel. The square cylinder was horizontally mounted on the mid-height of the end plates. Its axis was normal to the free stream and was 15.5D away from the leading edge of the end plates. The origin of the Cartesian coordinate system was chosen at the center of the square cylinder, and the x-axis, y-axis and z-axis were along the streamwise, vertical and spanwise directions, respectively. A slot spanning from z/D=-2.5 to 2.5 was disposed along the line y=0 on the upstream surface of the model. The slot had a width of w = 1 mm and was communicated with the cylindrical cavity. The diameter of the cavity was d=14 mm. One of its ends was closed and the other was designed as the inlet connecting with the synthetic jet excitation system.

A type of piston-driven synthetic jet actuator was used. A servo electromotor as well as an eccentric disk rotated uniformly under the control of computer. The circular motion was then converted into the reciprocating motion of the piston by a centric slider-crank mechanism. The outer diameter of the piston was D_p=29 mm. Since the piston cylinder was joint with the inlet of the square cylinder, the periodic injection and suction would be achieved for fluid inside the cavity of the square cylinder, generating the synthetic jet vortex pairs at the slot exit. The excitation frequency of synthetic jet was proportional to the rotating speed of the servo electromotor, which could be set via the control software on the computer.

The flow field was measured using a two-dimensional time-resolved particle image velocimetry system. The target field in the (x, y) plane was illuminated by a continuous laser sheet with wavelength of 532 nm and thickness of 1 mm. The particles used were the hollow glass beads with diameter of 5~20 μm and density of 1.05g cm^{-3}. The complementary metal-oxide-semiconductor (CMOS) cameras used have a gray level of 12 bits and a maximum spatial resolution of 2048 × 2048 pixels. Due to the

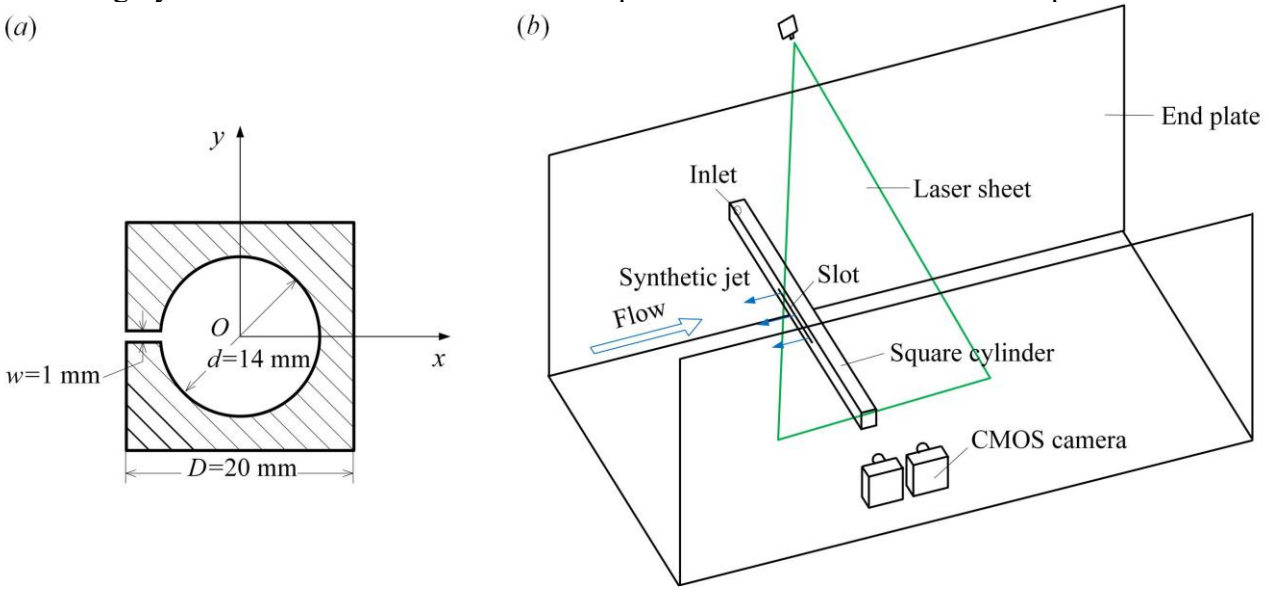

Fig. 1. (a) Cross-section of square cylinder and coordinate definition, (b) arrangement of experimental models and PIV system.

limitation of the shooting angle and the spatial resolution of camera, the flow field upstream and downstream of the square cylinder could not be captured by one camera at one time. Thus, two cameras were controlled by a synchronizer to record particle images upstream and downstream of the square cylinder simultaneously. The field of view (FOV) for the upstream camera was in the region of $-4 \le x/D \le 2$, $-2.75 \le y/D \le 2.75$, while the downstream FOV covered the area of $-1 \le x/D \le 11$, $-5.75 \le y/D \le 5.75$. 5457 snapshots were captured by one camera at one time. For each case, at least 10800 snapshots were used to get the statistics.

The velocity fields were calculated from the particle images using the multi-pass iterative Lucas-Kanade (MILK) algorithm, which has a high computational efficiency with GPU acceleration. Detailed descriptions about this algorithm can be found in Champagnat *et al*. (2011) [2] and Pan *et al*. (2015) [7]. For both the images upstream and downstream, the interrogation window for the last pass was 32 × 32 pixels with 75% overlap.

In the current experiment, the Reynolds number based on the free-stream velocity U_∞ and the side width D of the square cylinder was Re_D=1000. The flow behaviors for the natural case and a controlled case are compared. The excitation frequency f_e normalized by the natural shedding frequency f_0 was 0 and 3.4. The stroke length L_0 nondimensionalized by the slot width w was L_0/w=43.6 for the controlled case. The frame rates of the cameras for these two cases are 50 Hz and 150 Hz, respectively. The exposure time was no longer than 3.3 ms.

3 Experimental Results

For the controlled case of f_e/f_0=3.4, the synthetic jet injected from the slot keeps deflecting to one side (either $+y$ or $-y$ direction) and does not change the deflecting direction to the other side during the whole excitation process. The results give the examples that the synthetic jet deflects toward the $+y$ direction. The phase-averaged vorticity superimposed on the phase-averaged streamlines around the front and upside surfaces of the square cylinder is shown in Fig. 2. At the beginning of the blowing stroke, a pair of counter-rotating synthetic jet vortices generates at the exit of the slot due to the flow separation, the vortex pair grows gradually as it deflects. It is worth noticing that the upper clockwise vortex tends to move around the top-front corner of the square cylinder and has an obvious shift in y direction, while the location of the lower counter-clockwise vortex does not vary apparently. Since the blowing velocity at the slot exit is relatively high, the vortices subsequently lose the stability and break down, the disintegrated vorticity convects downstream under the driven of free stream.

The streamlines in Fig. 2 also show the variation of the separation region beside the upside surface. Influenced by the downwash of the upper synthetic jet vortex, the separation point on the upside is no longer fixed at the top-front corner but moves downstream with the convection of the synthetic jet. The separation region becomes much smaller and disappears with the decay of the synthetic jet vortices. To further illustrate this observation, the evolution of the time-averaged streamwise velocity $\overline{U}$ with phase in the range of $-0.5 \le x/D \le 0.5$ at $y/D = 0.625$ for the natural case and the controlled case is compared in Fig. 3. The regions inside the dash-dotted line represent the areas where $\overline{U}$ is less than 0. According to Huang *et al*. (2017) [4], the separation layers oscillate periodically due to the periodic shedding of wake vortices. Thus, the length of $\overline{U} < 0$ at a certain y location also oscillates with time, as shown in Fig. 3(*a*). While for the controlled case in Fig. 3(*b*), the area of $\overline{U} < 0$ shrinks significantly, and the midpoint of the line segment $\overline{U} < 0$ moves downstream with phase, which is consistent with the results observed in Fig. 2.

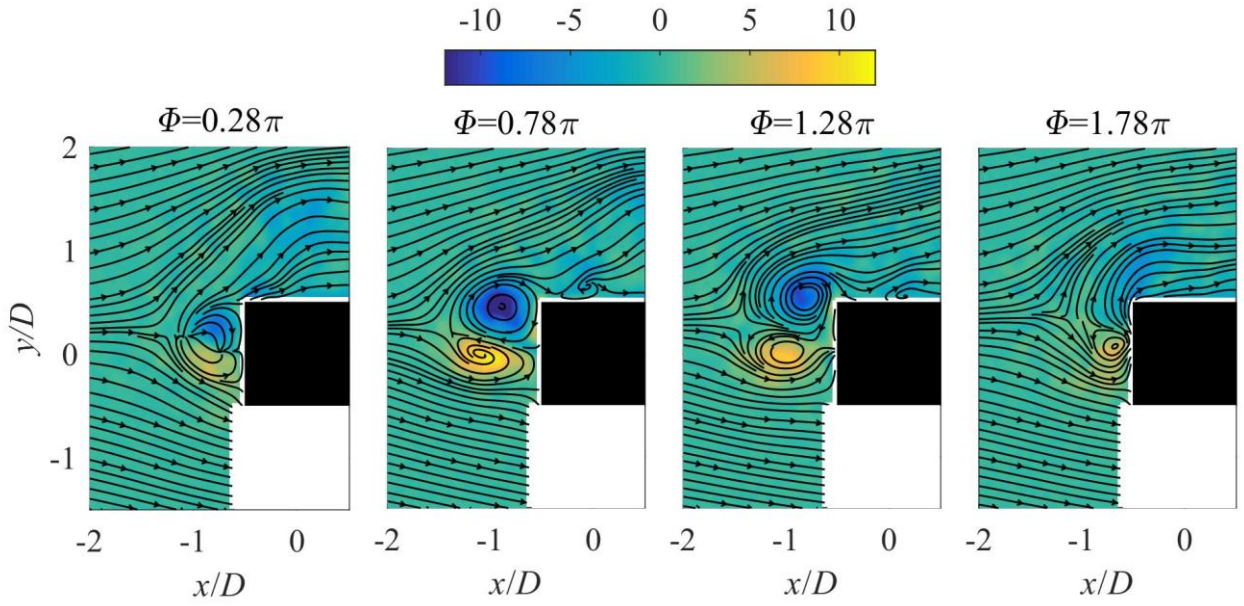

Fig. 2. Evolution of the phase-averaged vorticity $\omega D / U_\infty$ superimposed on the phase-averaged streamlines within one excitation cycle for f_e/f_0=3.4.

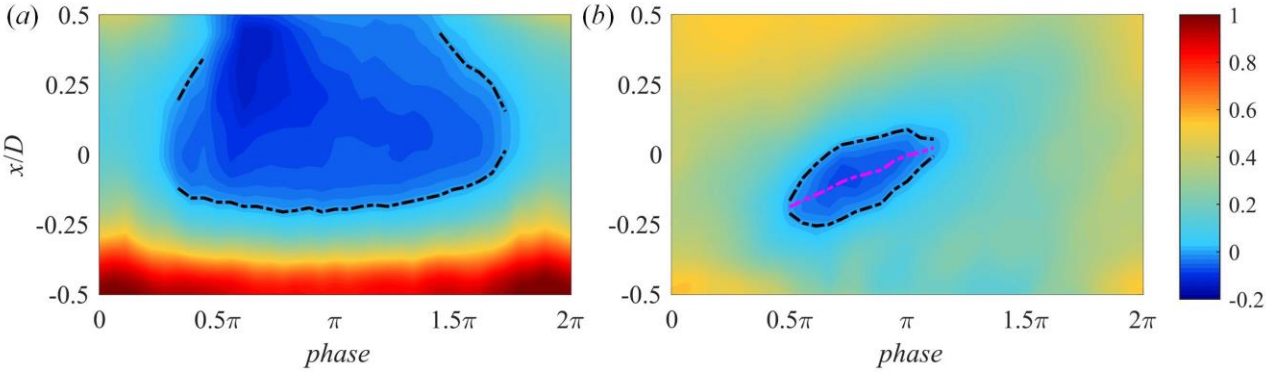

Fig. 3. Variation of the time-averaged streamwise velocity $\overline{U}$ with phase in the range of -0.5 ≤ x/D ≤ 0.5 at y/D = 0.625, (*a*) f_e/f_0=0, (*b*) f_e/f_0=3.4.

Fig. 4 demonstrates the time-averaged streamlines around the square cylinder. For the natural case (Fig. 4(*a*)), the streamlines approach the front corners after touching with the front surface of the square cylinder, and then flow separates at the front corners, forming separation regions between the shear layers and the side surfaces. The separation bubble downstream of the cylinder is symmetric about the centerline y/D=0. For f_e/f_0=3.4 (Fig. 4(*b*)), however, two counter-rotating recirculation regions, with the centerline above y=0 due to the deflection effect of the synthetic jet, are captured clearly at the upstream of the square cylinder, the front stagnation point is pushed more upstream by the synthetic jet. The centerline of the recirculation regions in the wake is below the line y=0. No obvious flow separation is observed beside the upside surface of the square cylinder from this time-averaged result.

The Fourier mode decomposition (FMD) method [6] is used to explore the frequency characteristics of the field at the upstream of the cylinder's rear surface. The calculation region for FMD analysis is in

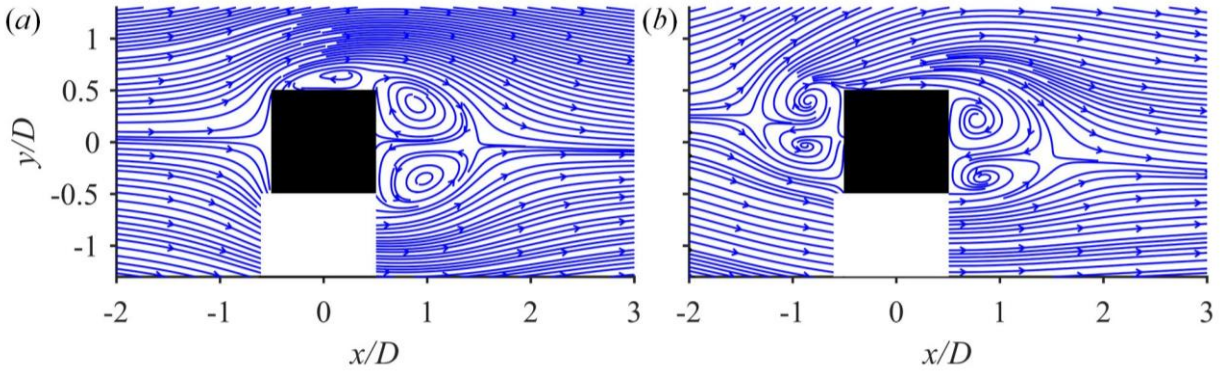

Fig. 4. Time-averaged streamlines around the square cylinder, (*a*) f_e/f_0=0, (*b*) f_e/f_0=3.4.

the range of -2.5 ≤ x/D ≤ 0.5, -2.5 ≤ y/D ≤ 2.5. The spectra are shown in Fig. 5. For the natural case, previous studies have found that the wake vortex shedding could change the behaviors of the boundary layers around the side surfaces, the influence could further be transferred to the flow field near the front surface [5]. This helps to explain the result that the dominant frequency resolved by FMD is the same as the wake vortex shedding frequency in Fig. 5(*a*). For the case of f_e/f_0=3.4, influenced by the periodic behavior of the synthetic jet, the upstream flow field is dominated by the excitation frequency of the synthetic jet.

As for the flow pattern in the wake, the Karman vortices shed alternatively from the shear layers when f_e/f_0=0. However, due to the disturbance brought by the synthetic jet in the upstream, the instantaneous flow field in the wake for the controlled case becomes turbulent, the distribution of the vorticity is messy, and the periodic evolution of wake vortices can not be observed in the current experiment. The Fourier mode decomposition is also conducted for the streamwise velocity signal in the wake field of 0.5 ≤ x/D ≤ 8, -3.5 ≤ y/D ≤ 3.5. As demonstrated in Fig. 6, the peak value is located at f/f_0=1 for the natural case, representing the wake vortex shedding frequency. However, no obvious peak is detected near the natural shedding frequency for f_e/f_0=3.4 with the current frame rate and sample length. A local peak is located at f/f_0=3.4, corresponding to the excitation frequency. Fig. 7 displays the FMD modes of the streamwise component with the frequency of 3.4f_0 for the case of f_e/f_0=3.4. It can be seen that the structures are mainly distributed in the upper side of the near wake, corresponding to the region that the dispersed synthetic jet flows through.

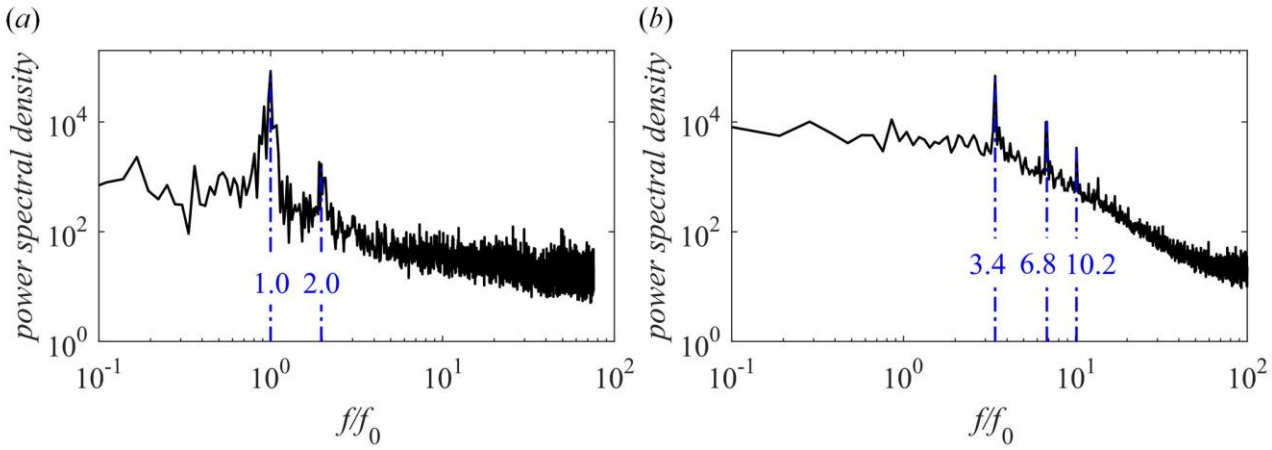

Fig. 5. FMD spectra of the upstream flow field for different cases, (*a*) f_e/f_0=0, (*b*) f_e/f_0=3.4.

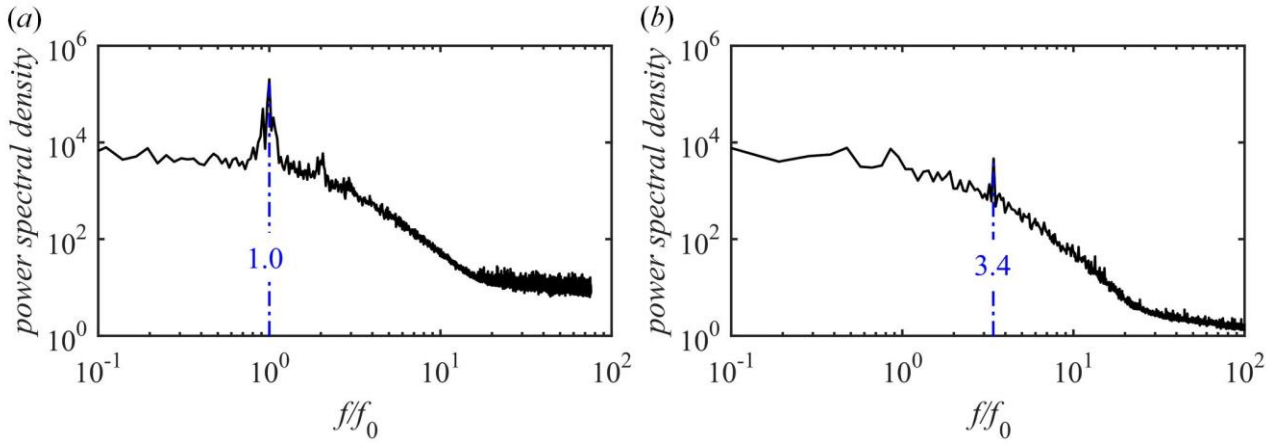

Fig. 6. FMD spectra of the flow field in the wake for different cases, (*a*) f_e/f_0=0, (*b*) f_e/f_0=3.4.

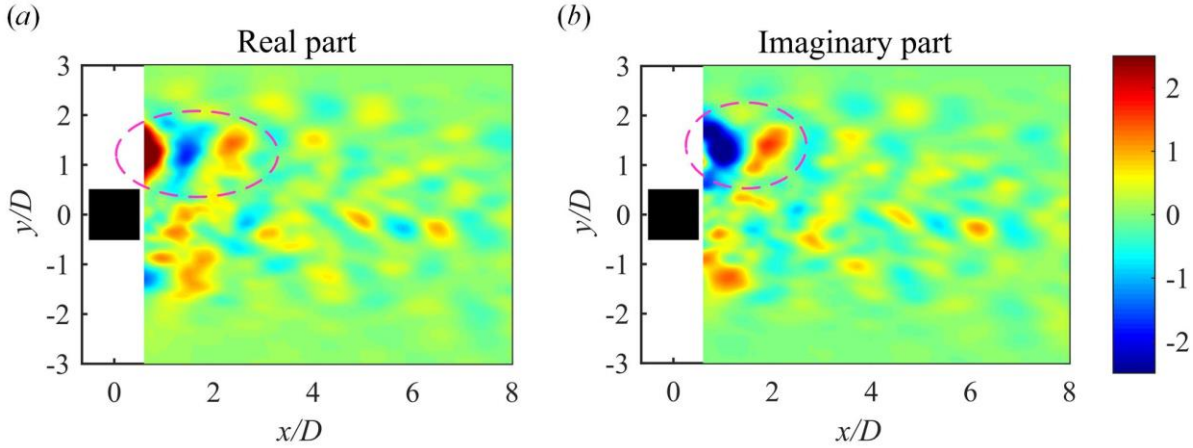

Fig. 7. Modes of streamwise component with the frequency of 3.4f_0 resolved by FMD for the case of f_e/f_0=3.4.

4 Conclusions

The flow behaviors around a square cylinder controlled by synthetic jet positioned at the upstream surface were investigated. The dimensionless excitation frequency was at a certain value of f_e/f_0=3.4. The two-dimensional time-resolved particle image velocimetry technique was used to get the velocity field. The synthetic jet keeps deflecting to one side (either $+y$ or $-y$ direction) during the whole excitation process. The phase-averaged results show that the synthetic jet vortices firstly grow and then disperse as they convect downstream. The separation beside the side surface where the synthetic jet deflects is suppressed effectively. Two counter-rotating recirculation regions are formed in the upstream of the square cylinder in the time-averaged flow field, and the recirculation regions in the wake become asymmetric about y=0 due to the deflection effect. According to the spectrum obtained by Fourier mode decomposition, the flow field at the upstream of the cylinder's rear surface is dominated by the excitation frequency of synthetic jet. No periodic wake vortex shedding is observed in the current experiment for f_e/f_0=3.4.

References

[1] Akansu Y E & Fırat E. Control of flow around a square prism by slot jet injection from the rear surface. *Exp. Therm. Fluid Sci.*, 34 (7), 906-914, 2010.

[2] Champagnat F, Plyer A, Le Besnerais G, Leclaire B, Davoust S. & Le Sant Y. Fast and accurate PIV computation using highly parallel iterative correlation maximization. *Exp. Fluids*, 50 (4), 1169–1182, 2011.

[3] Choi H, Jeon W P & Kim J. Control of flow over a bluff body. *Annu. Rev. Fluid Mech.*, 40, 113-139, 2008.

[4] Huang R F, Hsu C M & Chen Y T. Modulating flow and aerodynamic characteristics of a square cylinder in crossflow using a rear jet injection. *Phys. Fluids*, 29 (1), 015103, 2017.

[5] Huang R F, Hsu C M & Chiu P C. Flow behavior around a square cylinder subject to modulation of a planar jet issued from upstream surface. *J. Fluids Struct.*, 51, 362-383, 2014.

[6] Ma L Q, Feng L H, Pan C, Gao Q & Wang J J. Fourier mode decomposition of PIV data. *Sci. China Technol. Sci.*, 58 (11), 1935–1948, 2015.

[7] Pan C, Xue D, Xu Y, Wang J J & Wei R J. Evaluating the accuracy performance of Lucas–Kanade algorithm in the circumstance of piv application. *Sci. China Phys. Mech. Astron.*, 58 (10), 1–16, 2015.

[8] Qu Y, Wang J J, Sun M, Feng L H, Pan C, Gao Q & He G S. Wake vortex evolution of square cylinder with a slot synthetic jet positioned at the rear surface. *J. Fluid Mech.*, 812, 940-965, 2017.

[9] Saha A K & Shrivastava A. Suppression of vortex shedding around a square cylinder using blowing. *Sadhana*, 40 (3), 769-785, 2015.

Copyright Statement

The authors confirm that they, and/or their company or institution, hold copyright on all the original material included in their paper. They also confirm they have obtained permission, from the copyright holder of any third-party material included in their paper, to publish it as part of their paper. The authors grant full permission for the publication and distribution of their paper as part of the ISFV18 proceedings or as individual off-prints from the proceedings.